J Mater Sci (2020) 55:10765–10772

Energy materials

Semimetal Bi/carbon fibers derived from electrospinning polyacrylonitrile and its visible light photocatalytic performance

Danfeng Zhang[1], Zeyu Xu[2,3,*], Huan Zhao[2], Tong Liu[1], Changwei An[1], and Jianguo Liu[2,*]

[1] School of Biomedical and Chemical Engineering, Liaoning Institute of Science and Technology, Benxi 117004, China
[2] Institute of Metal Research, Chinese Academy of Sciences, Shenyang 110016, China
[3] School of Materials Science and Engineering, University of Science and Technology of China, Shenyang 110016, China

Received: 9 March 2020
Accepted: 16 April 2020
Published online: 1 May 2020

ABSTRACT

A series of semimetal Bi-doped carbon fibers (Bi/CFs) were prepared by electrospinning-calcined polyacrylonitrile technique and characterized by XRD, SEM, EDS, XPS and UV–Vis DRS spectra to probe the morphology, structure and optical properties. Then, the Bi/CFs hybrids as photocatalysts were investigated the photocatalytic performances for degradation of representative environmental contaminants (Congo red dye and antibiotics sulfanilamide) under visible light irradiation ($\lambda > 420$ nm). In different compositions, the photocatalytic efficiencies have followed the order as Bi (5%)/CFs > Bi (10%)/CFs > Bi (1%)/CFs > polyacrylonitrile carbon fibers, that was mainly for the surface plasmon resonance effect of semimetal Bi, which made Bi/CFs hybrids had high light-harvesting properties and effective separation abilities of photogenerated carriers. According to the results of optical performance and the scavengers trapping experiments, the feasible photocatalytic mechanism was deduced. This study provided semimetal Bi, a new plasmonic co-catalyst, as a well substitute for Au and Ag noble metal to be a promising potential for environmental contaminants treatment.

Introduction

Nowadays, in the wake of rapid development of economy and industry, environmental water contamination issues became one of the intractable problems all over the world [1]. Photocatalytic water purification was a green and effective technology to treatment of water pollutants, which utilized inexhaustible solar energy [2, 3]. Therefore, development of various of photocatalysts became the focus for more and more researchers [4–6].

Surface plasmon resonance (SPR) effect of noble metal was deemed to be an effective means for photocatalytic remediation of environmental pollutant

Address correspondence to E-mail: zyxu16s@imr.ac.cn; jgliu@imr.ac.cn

https://doi.org/10.1007/s10853-020-04696-2

[7–10]. Au, Ag and Pt were widely used as co-catalyst for photocatalysis due to their SPR effect [11–14]. While in view of the over-expenditure for water treatment, inexpensive and eco-friendly metals were sought to replace of these noble metals. Recently, a typical semimetal material bismuth (Bi) draws attentions because of its non-toxic, green, high carrier motility and low cost [15–17]. It was found that semimetal Bi was an attractive plasmonic photocatalyst and can act as the good substitute of the noble metal. For example, Zhu et al. obtained C/Bi/Bi_2O_3 composite by calcining the precursor to photocatalytic degradation of 2,4-dichlorophenol [18]. Chiu et al. found that Bi/C/α-Bi_2O_3 prepared by thermal decomposition exhibited superior photocatalytic activity for MO and MG degradation under visible light irradiation [19]. Bi microsphere/g-C_3N_4 was synthesized and used for photocatalytic H_2 evolution and NO removal under visible light irradiation [16, 20]. Nevertheless, as far as we know, doping semimetal Bi with carbon fibers by electrospinning of polyacrylonitrile and its photocatalytic performance have no other report.

Herein, a series of semimetal Bi coupling with carbon fibers derived from electrospinning of polyacrylonitrile were prepared and the photocatalytic activities were investigated by degradation of environmental water contaminants including dye (Congo red) and antibiotics (sulfanilamide) under visible light irradiation. Based on the trapping experiments, the possible photocatalytic mechanism of Bi/CFs was speculated.

Experimental section

Synthesis of Bi/CFs hybrids

The formation process of Bi/CFs hybrids is demonstrated in Scheme 1 in detail. Typically, the carbon nanofiber webs were woven by electrospinning method. Firstly, the precursor solution containing 16wt% solute was obtained by mixing polyacrylonitrile (PAN, M_w = 90,000) with *N*–*N*-dimethylformamide (DMF) solvent at 70 °C. Then, it was separated° into four bottles, each containing 30 mL. After that, $BiCl_3$ of 0.48 g, 0.24 g and 0.048 g were, respectively, added into four bottles under vigorous stirring. The uniform mixed solution was loaded into a syringe equipped with an 18G stainless steel needle. A high voltage (21 kV) was applied to the needle, and the solution was propelled at a speed of 3 mL h^{-1}. Besides, the rotating speed of collecting drum was 300 rpm and the distance between the needle and collecting drum was 20 cm. The prepared nanofiber webs were pre-oxidized in a tubular furnace for 30 min in the air and then carbonized at 1000 °C for 1.5 h in nitrogen atmosphere with a heating rate of 5 °C min^{-1}. Then, the products named Bi (10%)/CFs, Bi (5%)/CFs, Bi (1%)/CFs, respectively, were obtained.

Characterization

Scanning electron microscopy (SEM) (FEI INSPECT-F, USA) was used to detect the morphology of the materials. X-ray diffraction (XRD) patterns with diffractometer D8 (Bruker AXS, Germany) were performed in the range of 2θ = 10°–80°. An ESCAlab 250Xi electron spectrometer from Thermo Scientific (300 W Al Kα radiations) was investigated X-ray photoelectron spectroscopy (XPS). A Metash UV-8000S with $BaSO_4$ as the reflectance standard recorded the UV–visible diffuse reflectance spectra (DRS).

Photocatalytic experiments

The photocatalytic properties of the hybrids were investigated by photodegradation of target contaminant (Congo red (CR) dye or sulfanilamide (SA) antibiotics) under visible light using 300 W Xe lamp (PLS-SXE300, Beijing Perfect Light) with UV-cutoff filter ($\lambda > 420$ nm). Typically, 0.5 g L^{-1} of the sample was added to 50 mL of target contaminant aqueous solution (10 mg L^{-1}) under vigorous stirring. Before irradiation, the suspension was kept in dark for 30 min with continuous stirring to achieve adsorption–desorption equilibrium. In the process of visible light irradiation, 3 mL aliquots were sampled at a certain interval of time and removed the catalysts by centrifugation. Then, the concentration of target contaminant aqueous solution was monitored by UV–Vis spectrophotometer.

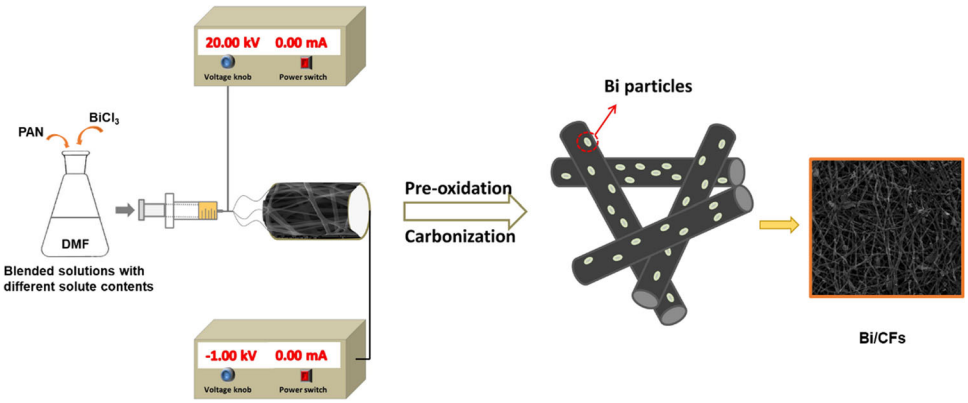

Scheme 1 Illustration for the formation process of Bi/CFs hybrids.

Results and discussion

Characterization

Figure 1 shows XRD patterns of the as-prepared samples to characterize the phase and the structure. Figure 1a suggests that two diffraction peaks were at 2θ = 15.68° and 22.61°, which referred to the lateral packing of crystalline regions in PAN molecules. Also, a weak and wide peak located at about 42.3° corresponded to (100) characteristic reflection peak of carbon materials, indicating that the spun nanofibers were completely carbonized with the carbonization temperature over 1000 °C [21, 22]. As displayed in Fig. 1b–d, it can be found that the two peaks located at 10°–25° belong to the characteristic peaks of PAN-C. Then, the diffraction peaks at 27.81°, 37.60°, 39.87°, 48.49° and 64.16° were well matched with the (012), (104), (110), (202) and (122) planes of semimetal Bi (JCPDS No. 44-1246) [16], illustrating that semimetallic Bi was doped on carbon fibers.

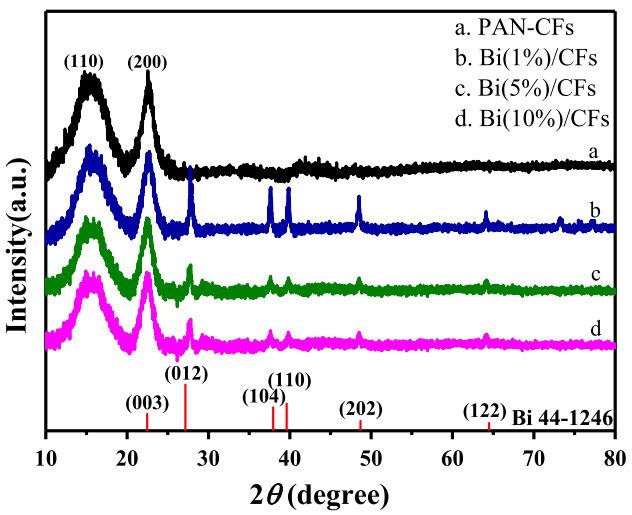

Figure 1 XRD patterns of different samples.

Figure 2a displays the SEM image of carbon fibers formed by electrostatic spinning of polyacrylonitrile, which had a diameter in the range of 300–500 nm, and the surface was smooth without other impurity. The smooth surface of PAN-CFs (inset of Fig. 2a) can be attributed to the carbonized procedure and the high calcined temperature to 1000 °C. As displayed in image of Fig. 2a, b–d, mass of Bi spheres in situ grew on the surface of PAN-CFs with different Bi-doped contents from 1 to 10%. From the image of inset of Fig. 2c, the diameter of Bi microsphere was approximately 1–2 μm. It can be found that Bi microspheres were uniformly immobilized on the surface of PAN-CFs. In Fig. 2d, as the Bi-doped content increased to 10%, many Bi microspheres agglomerated severely each other, which will hinder the active sites and affect the photocatalytic activity. The corresponding EDS mapping images of Bi (5%)/CFs sample clearly demonstrated the homogeneous spatial distribution of C, O, Bi elements (Fig. 2e).

The elemental and chemical states of Bi/CFs hybrid were investigated by XPS spectra (Fig. 3). Figure 3a exhibits all of the detected elements of PAN-CFs and Bi (10%)/CFs in survey XPS spectra. It was noted that the existence of N in the survey spectra was probable due to nitrogen contamination species from XPS measurement and the N_2 calcination process. From Fig. 3b, c, the peak of C 1 s at binding energy 283.6 eV shifted to 281.4 eV and the peak of O 1 s at 530.8 eV shifted to 528.7 eV. Apparently, blueshift happened after doping Bi, indicating the interaction between semimetallic Bi microspheres and PAN-CFs. As shown in Fig. 3d, two peaks at binding energy of 164.4 eV and 161.3 eV belong to Bi–Bi bond of semimetallic Bi microsphere.

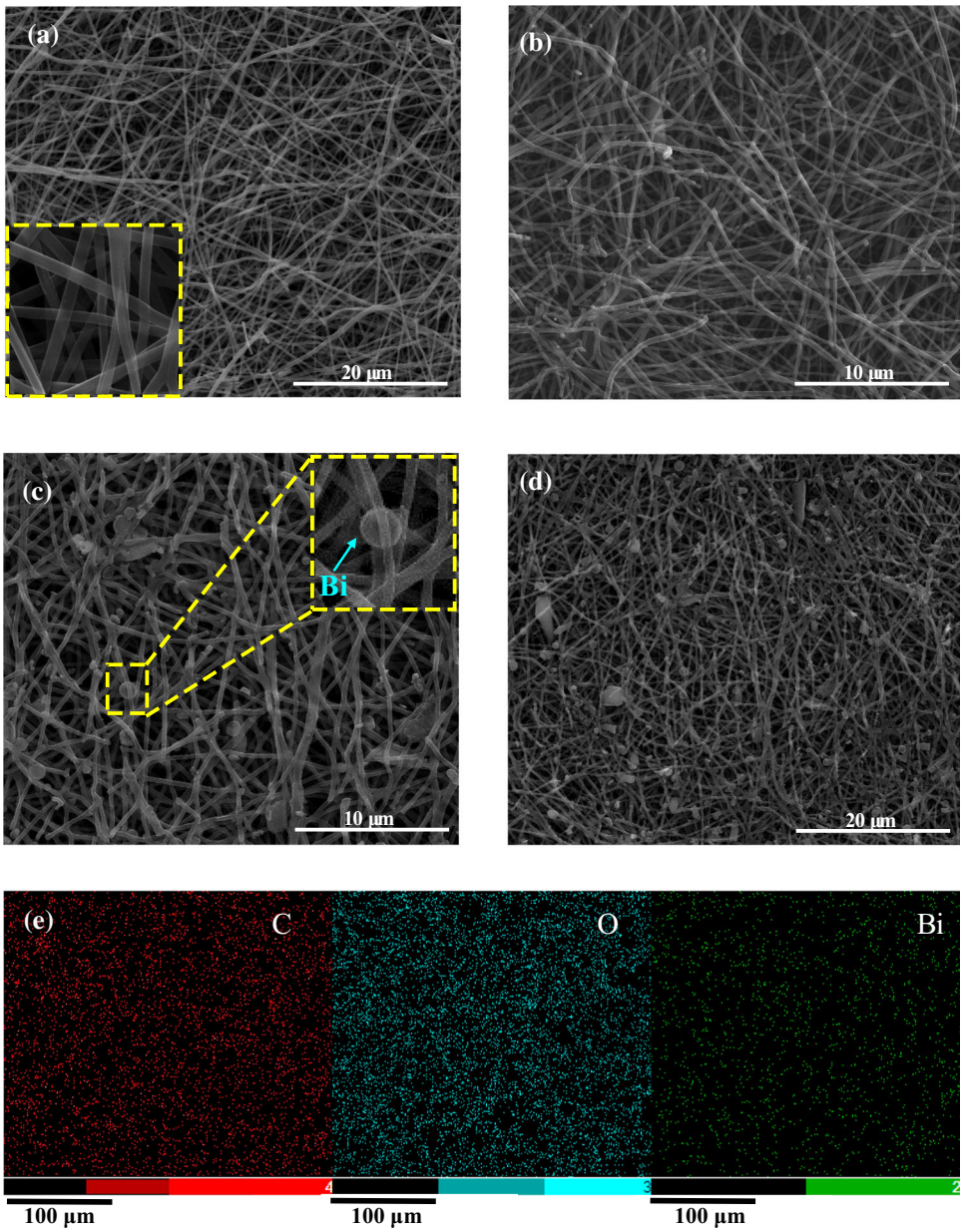

Figure 2 SEM images of **a** carbon fibers, **b** Bi (1%)/CFs, **c** Bi(5%)/CFs, **d** Bi(10%)/CFs (inset image was the part enlargement) and **e** the corresponding C, O, Bi elements in EDS mapping of Bi(5%)/CFs sample.

In consequence, XPS results further verified the existence of the elements in Bi/CFs hybrids, which was in accordance with EDS.

Figure 4 illustrates the UV–Vis DRS of PAN-CFs and different content Bi/CFs hybrids. Compared with PAN-CFs, the light adsorption capability was conspicuously heightened from 400 to 800 nm after Bi doped. That was mainly because of the charge-transfer transition between Bi microspheres and PAN-CFs. Furthermore, Bi/CFs hybrids demonstrated wide absorption peak over 500–600 nm, which was the obvious characteristic SPR peak of semimetal Bi [20, 23]. The enhanced light adsorption ability was inevitably in favor of prompting photoexciting electron–holes to improve the photocatalytic performance of Bi/CFs hybrids.

Photocatalytic capabilities of Bi/CFs hybrids

The photocatalytic performances of Bi/CFs hybrids were evaluated by degradation CR dye solution and antibiotic SA solution under visible light irradiation in 120 min. As shown in Fig. 5a, the photodegradation of CR dye was almost negligible in 120 min without any catalyst under visible light irradiation ($\lambda > 420$ nm). In the same way, the PAN-CFs as the

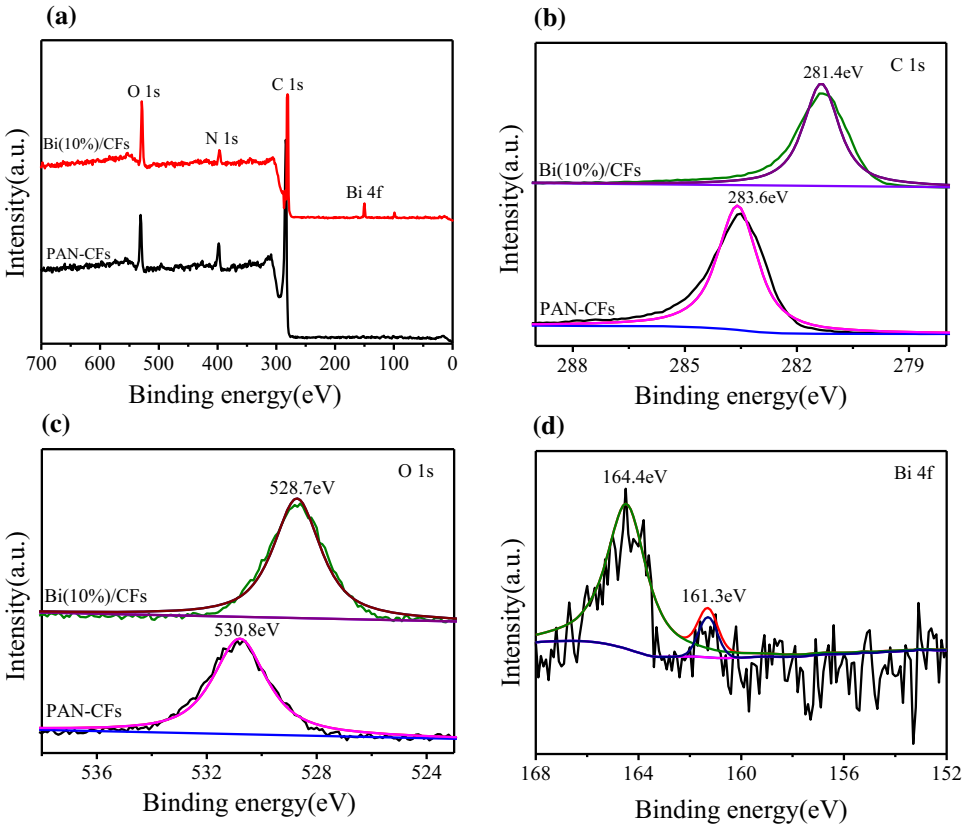

Figure 3 XPS spectra, **a** survey of Bi(10%)/CFs and PAN-CFs, **b** C1s spectra of Bi(10%)/CFs and PAN-CFs, **c** O1s spectra of Bi(10%)/CFs and PAN-CFs and **d** Bi 4f spectrum of Bi(10%)/CFs.

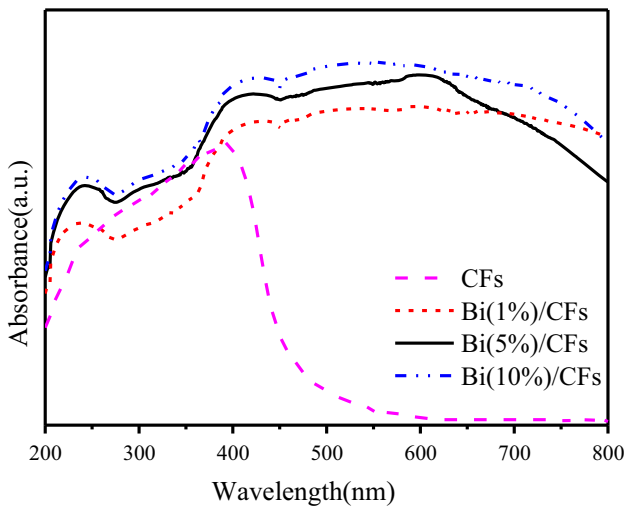

Figure 4 UV–Vis DRS of different Bi/CFs samples.

catalyst gave poor photodegraded activity. However, a series of Bi/CFs hybrids, including Bi (1%)/CFs, Bi (5%)/CFs and Bi (10%)/CFs, exhibited satisfied degradation capacities. The superior photocatalytic activity of Bi/CFs hybrids may be attributed to SPR effect of semimetal Bi doped with PAN-CFs and the visible light absorption capability of PAN-CFs [18]. Bi (5%)/CFs illustrated the highest photocatalytic performance (97.2% degradation efficiency) than Bi (1%)/CFs (67.1%) and Bi (10%)/CFs (89.4%). When the content of semimetal Bi increased in the hybrid, excessive Bi will serve as the mediators for recombination of photoinduced carriers, which brought down the photocatalytic activity [24]. Figure 5b displays similar photocatalytic tendency for degradation of antibiotic SA solution.

Figure 6a illustrates the result of four recycle runs for degradation of CR and SA over Bi (5%)/CFs hybrid under the same experimental conditions. It was obvious that, after four runs, insignificant more decrease for degradation efficiency in photocatalytic activity was found. That may be a bit of loss during wash-dry circulation process. Namely, the Bi (5%)/CFs hybrid was stable and prospective for environmental wastewater treatment under visible light irradiation.

Deduced photocatalytic mechanism

To further explore the active species and deduce the photocatalytic mechanism, the trapping experiments

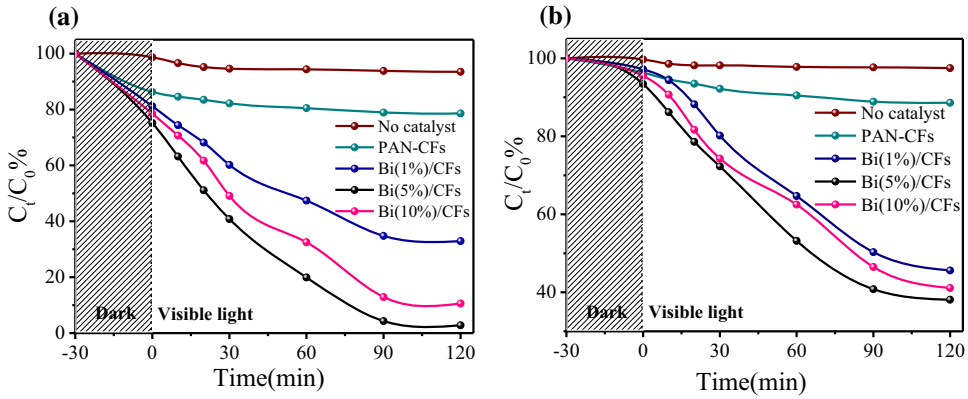

Figure 5 Photocatalytic degradation of **a** CR and **b** SA over different catalysts under visible light irradiation in 120 min.

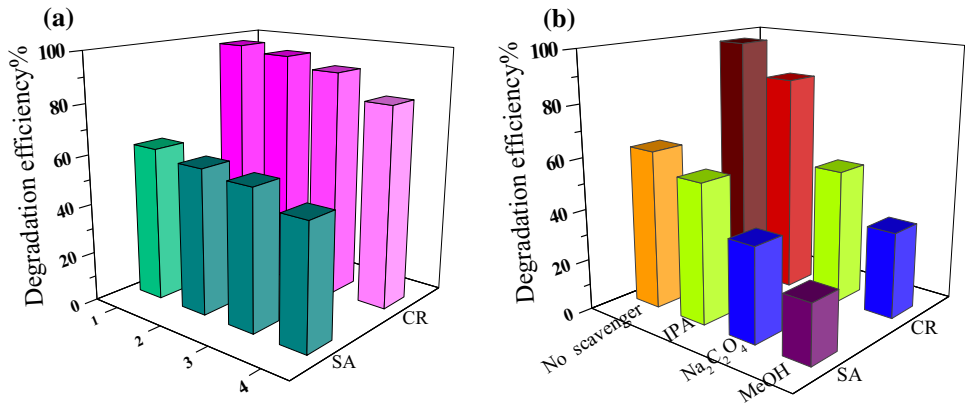

Figure 6 **a** Recycling properties over Bi (5%)/CFs for CR and SA degradation under visible light irradiation; **b** the influence of different scavengers on the photodegradation of CR and SA over Bi (5%)/CFs.

were performed. Different scavengers, $Na_2C_2O_4$ served as hole (h^+) scavenger [25], isopropanol (IPA) and methyl alcohol (MeOH) act as ·OH and $\cdot O_2^-$ scavenger [26, 27], were used in the photodegradation reaction. As shown in Fig. 6b, with the introduction of IPA, the degradation efficiency of CR/SA decreased a little. However, the degradation efficiency of CR/SA was remarkably hampered as MeOH was introduced into the system. When $Na_2C_2O_4$ was introduced, a certain repression was also found. That manifested that $\cdot O_2^-$ radical was the main active species as well as h^+ was subordinate active species for the whole degradation process.

According to the whole experimental results, the schematically deduced photocatalytic mechanism is demonstrated in Scheme 2. A survey of the previous literature showed that semimetal Bi had surface plasmon effect which facilitated the separation of photogenerated electron–holes. Under the visible light irradiation, the hot electrons (e^-) can be aroused and emitted from the materials due to the SPR of semimetal Bi. Then, the hot electrons will transfer quickly from SPR Bi materials to the PAN-CFs, leaving positive charges (h^+) on E_f (− 0.17 eV) [28]. Ultimately, the e^- transferred to the surface of PAN-CFs will accept O_2 to form $\cdot O_2^-$ radical, and the h^+ oxidized H_2O molecular to ·OH, which effectively inhibited the recombination of e^-/h^+ pairs. As we know, the semimetal Bi can perform as electron traps to accelerate the separation of photogenerated e^-/h^+ pairs. Then, a number of pollutant molecules (CR dye or SA antibiotics) absorbed on the surface of Bi/CFs were oxidized by active species $\cdot O_2^-$, h^+ and ·OH to decompose step by step.

Comparing with other photocatalysts

The photocatalyst Bi/CFs hybrid was compared to other photocatalysts for determination of the photocatalytic capability from the viewpoint of preparation methods, type of target pollutants and degradation efficiency (Table 1). Due to the special SPR effect of semimetal Bi, Bi/CFs hybrid processed high light-harvesting properties and effective separation abilities of photogenerated carriers, which result in satisfied photocatalytic performance. It was further evidenced that the photocatalyst Bi/CFs had

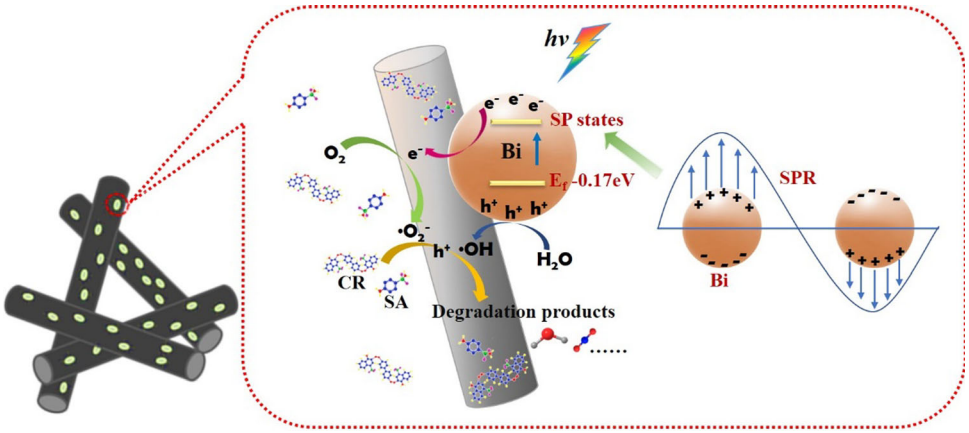

Scheme 2 Schematic photocatalytic mechanism of Bi/CFs under visible light.

Table 1 A comparison with other catalysts for determination of catalytic ability

Catalyst[a]	Method	Target pollutants[b]	Degradation efficiencies%	References
N-doped TiO_2	Sol–gel with one-pot method	o-phenylphenol	46	[29]
C/Bi/α-Bi_2O_3	Calcining in N_2	MO and MG	93 and 82	[19]
Ni–$BaMo_3O_{10}$	Microwave hydrothermal method	IC	98	[30]
g-CN/Au–SQD	Sonication–stirring–annealing	RhB	99	[31]
Bi/CFs	Electrospinning calcined	SA and CR	97.2 and 61.9	This work

[a]*g-CN/Au-SQD* g-C_3N_4/Au-SnO_2 quantum dot

[b]*MO* methyl orange, *MG* malachite green, *IC* indigo carmine, *RhB* rhodamine B

promising potential applications for eliminating various organic contaminants.

Conclusion

Summarily, a series of Bi/CFs were prepared by electrospinning technique as photocatalyst, which exhibited outstanding photocatalytic performance for degradation of Congo red dye and antibiotics sulfanilamide under visible light ($\lambda > 420$ nm), that mainly belongs to the special SPR effect of semimetal Bi. The hybrids Bi/CFs not only had favorable light-harvesting ability, but also possessed higher separation capability of photogenerated carriers. This work provided a new sight for nonmetallic material as the expensive plasmonic catalyst Au or Ag substitute in environmental contamination remediation.

Acknowledgements

This project was supported by the Doctoral Start-up Foundation of Liaoning Provincial Natural Science Foundation of China (2019-BS-129, 2019-BS-128), the Doctoral Start-up Foundation of Liaoning Institute of Science and Technology (Nos. 1810B07, 1810B09) and the Scientific Foundation Project of Education Department of Liaoning Province (L2019lkyjc-02). The authors also thank their colleagues who participated in this work.

Author contributions

DFZ and JGL conceived and designed the study. ZYX, TL and CWA performed the experiments. DFZ and HZ wrote the paper. DFZ, ZYX, HZ, TL, CWA and JGL reviewed and edited the manuscript. All authors read and approved the manuscript.

Compliance with ethical standards

Conflict of interest The authors declare that they have no conflict of interest.

References

[1] Rodriguez-Narvaez OM, Peralta-Hernandez JM, Goonetilleke A, Bandala ER (2017) Chem Eng J 323:361–380

[2] You J, Guo Y, Guo R, Liu X (2019) Chem Eng J 373:624–641

[3] Bolisetty S, Peydayesh M, Mezzenga R (2019) Chem Soc Rev 48:463–487

[4] Wang Z, Li C, Domen K (2019) Chem Soc Rev 48:2109–2125

[5] Yang WT, Liu XL, Li D, Fan LZ, Li YC (2015) Phys Chem Chem Phys 17:14532–14541

[6] Liu XL, Li D, Yang WT, Tang SL, Li XH, Fan LZ (2016) YC Li. J Mater Sci 51:11021–11037

[7] Hou W, Cronin SB (2013) Adv Funct Mater 23:1612–1619

[8] Wu N (2018) Nanoscale 10:2679–2696

[9] Wang M, Ye M, Iocozzia J, Lin C, Lin Z (2016) Adv Sci 3:1600024

[10] Shahzad A, Kim W-S, Yu T (2016) Dalton T 45:9158–9165

[11] Zhang W, Hu Y, Yan C et al (2019) Nanoscale 11:9053–9060

[12] Xu B, Li Y, Gao Y et al (2019) Appl Catal B-Environ 246:140–148

[13] Yang X, Liu S, Li J, Chen J, Rui Z (2020) Chemosphere 249:126096

[14] Fang J, Chen X, Wu Y, Liu H (2020) J Mater Sci 55:5880–5891

[15] Li J, Zhang W, Ran M, Sun Y, Huang H, Dong F (2019) Appl Catal B-Environ 243:313–321

[16] Dong F, Zhao Z, Sun Y, Zhang Y, Yan S, Wu Z (2015) Environ Sci Technol 49:12432–12440

[17] Hua C, Dong X, Wang Y, Zheng N, Ma H, Zhang X (2019) J Mater Sci 54:9397–9413

[18] Hao Q, Wang R, Lu H et al (2017) Appl Catal B-Environ 219:63–72

[19] Ma Y, Han Q, Chiu T-W, Wang X, Zhu J (2020) Catal Today 340:40–48

[20] Wei Z, Liu J, Fang W et al (2019) Chem Eng J 358:944–954

[21] Song C, Wang T, Qiu Y, Qiu J, Cheng H (2009) J Porous Mat 16:197–203

[22] Miao F, Shao C, Li X, Wang K, Liu Y (2016) J Mater Chem A 4:4180–4187

[23] Yu Y, Cao C, Liu H et al (2014) J Mater Chem A 2:1677–1681

[24] Weng S, Chen B, Xie L, Zheng Z, Liu P (2013) J Mater Chem A 1:3068–3075

[25] Wu Y, Li Y, Fang C, Li C (2019) ChemCatChem 11:2297–2303

[26] Tan L, Yu C, Wang M et al (2019) Appl Surf Sci 467–468:286–292

[27] Zeng L, Xiao L, Shi X, Wei M, Cao J, Long Y (2019) J Colloid Interf Sci 534:586–594

[28] Dong F, Li Q, Sun Y, Ho W-K (2014) ACS Catal 4:4341–4350

[29] Fiorenza R, Di Mauro A, Cantarella M et al (2020) Mat Sci Semicon Proc 112:105019–105025

[30] Ray SK, Dhakal D, Lee SW (2020) Mat Sci Semicon Proc 105:104697–104706

[31] Babu B, Koutavarapu R, Shim J, Yoo K (2020) Sep Purif Technol 240:116652–116667